Line strength factors for E,F$^1\Sigma_g^+(v' = 0, J' = J'')$ – X$^1\Sigma_g^+$ (v'', J'') (2 + 1) REMPI transitions in molecular hydrogen[1]

Andrew E. Pomerantz, Florian Ausfelder, Richard N. Zare, and Winifred M. Huo

Abstract: Experimentally and theoretically determined line strengths are presented for E,F$^1\Sigma_g^+(v' = 0, J' = J'')$ – X$^1\Sigma_g^+$ (v'', J'') (2 + 1) REMPI transitions in H_2, HD, and D_2. The experimental technique employs a hot filament source of internally excited hydrogen that allows experimental determination of line strengths for the low rotational states of highly excited vibrational manifolds ($v'' \leq 4$). The line strengths are found to depend only weakly on J'' for the states measured here, and theoretical results indicate that the line strengths depend strongly on v''. These values are combined with previously measured and calculated line strengths for these transitions (K.-D. Rinnen, M.A. Buntine, D.A.V. Kliner, R.N. Zare, and W.M. Huo. J. Chem. Phys. **95**, 214 (1991)), resulting in a more complete compilation of REMPI line strengths for molecular hydrogen.

Key words: hydrogen, spectroscopy, REMPI, line strength, multiphoton.

Résumé : Nous avons déterminé théoriquement et expérimentalement les forces de raies pour les transitions REMPI E,F$^1\Sigma_g^+(v' = 0, J' = J'')$ – X$^1\Sigma_g^+(v'', J'')$ (2 + 1) de H_2, HD et D_2. La technique expérimentale, qui utilise un filament chauffé comme source d'hydrogène rovibrationnellement excité, permet de mesurer les forces de raies pour les états rotationnels bas des niveaux vibrationnels excités ($v'' \leq 4$). Nos mesures montrent que les forces de raies ne dépendent que faiblement de J'', et les résultats théoriques indiquent que les forces de raies dépendent fortement de v''. Ces valeurs sont combinées aux forces de raies mesurées et calculées antérieurement pour ces mêmes transitions (K.-D. Rinnen, M.A. Buntine, D.A.V. Kliner, R.N. Zare, and W.M. Huo. J. Chem. Phys. **95**, 214 (1991)), ce qui conduit à une compilation plus complète des forces de raies REMPI pour l'hydrogène moléculaire.

Mots clés : hydrogène, spectroscopie, REMPI, force de raie, multiphoton.

Introduction

The electronic spectroscopy of molecular hydrogen has been studied extensively over the past century, beginning with the measurement of emission spectra by Lyman (1) and Werner (2). The classic investigation by Herzberg and Howe (3) on the H_2 B–X system exemplified the richness of information that can be obtained from photographic spectroscopy. More recent work has employed laser-based techniques that sacrifice the ability to observe many transitions simultaneously while allowing quantitative measurements of quantum state selective molecular concentrations. In particular, rovibrational state selective populations of hydrogen molecules resulting from gas-phase chemical reactions (4–7) or gas-surface interactions (8–10) have been studied using resonant enhanced multiphoton ionization (REMPI). The interpretation of experimental data requires an understanding of the relationship between the measured signals (ion currents) and populations of rovibrational states. Accurate line strengths for these REMPI transitions are essential for performing this transformation.

Most previous attempts to measure state specific concentrations of molecular hydrogen using REMPI have employed Q-branch members of the E,F$^1\Sigma_g^+$ – X$^1\Sigma_g^+$ transitions. Pożgainer et al. (11) have measured line strengths for the (0,0) and (1,1) transitions by analyzing state distributions produced by a Knudsen source. Marinero et al. (4) have measured line strengths for the (0,1) and (0,2) transitions in HD by calibrating against a rotationally relaxed microwave discharge source. Rinnen et al. (12) have employed a hot nozzle source to measure line strengths for these (0,0), (0,1), and (0,2) transitions in H_2, HD, and D_2. They were able to measure line strengths for 102 rovibrational levels, typically including Q(0)–Q(15) for each molecule at each vibrational level, although they were unable to determine line strengths for the low J'' levels of the $v'' = 1, 2$ manifolds. Huo et al.

Received 19 December 2003. Published on the NRC Research Press Web site at http://canjchem.nrc.ca on 19 June 2004.

A.E. Pomerantz, F. Ausfelder, and R.N. Zare.[2] Department of Chemistry, Stanford University, Stanford, CA, 94305–5080 USA.
W.M. Huo. NASA Ames Research Center, Mail Stop T27B-1, Moffett Field, CA, 94035–1000 USA.

[1]This article is part of a Special Issue dedicated to the memory of Professor Gerhard Herzberg.
[2]Corresponding author (e-mail: zare@stanford.edu).

 doi: 10.1139/V04-074

(13) have performed calculations using adiabatic potentials and summing of 124 intermediate states to provide theoretical values for these same line strengths.

The conclusions of these studies were that experiment and theory agreed very well and that the line strengths depend strongly on v'' but only weakly on J''. For each isotope, the experimentally determined line strengths increase with v'' up to $v'' = 2$, but calculations predict the line strengths to decrease sharply for higher v''. Line strengths typically increase slowly with J'' (constant to within 10% for the first 10 J'' states) although there are some deviations starting at $J'' = 12$ for H_2, 17 for HD, and 24 for D_2, arising from resonant tunneling between the two wells of the E,F state at high J'' levels (14).

Here we present relative line strengths measured using a hot filament source and absolute values of the square of the two-photon transition moment calculated using previously described theoretical methods (13). The measurements are sensitive to line strengths for the low-lying rotational states of $v'' = 1$–4 in HD and D_2 and of $v'' = 1$–3 in H_2. For completeness, the previously determined line strengths are also presented.

Experimental methods

The line strength measurements require a source of internally excited hydrogen with two characteristics: there must be sufficiently high concentrations in internally excited states as to allow detection, and the relative concentrations of each excited state must be known. Relative line strengths are then determined by comparing the measured concentration to the concentration the source is known to produce; if the measured concentrations equal the known concentrations for a given set of states, then the line strengths are constant within the experimental error for transitions originating from those states. The source of internal excitation of hydrogen used in this measurement is a hot filament. This hot filament promotes recombination reactions that populate excited states of molecular hydrogen, and the excited products can be rotationally but not vibrationally relaxed by collisions before detection. This technique has been shown previously to produce high concentrations of vibrationally excited hydrogen that is rotationally thermalized to slightly above room temperature (15–18).

The filament used in this experiment is the tungsten filament of a nude ionization gauge (Granville Phillips 274-025 gauge with series 330 controller). The ion gauge is operated with an emission current of 10 mA, and the flow of hydrogen is metered with a dual-stage micrometer valve to maintain a nominal pressure of 9×10^{-5} to 10×10^{-5} torr (1 torr = 133.322 Pa) in the ion gauge during the course of an experiment. The chamber walls immediately surrounding the filament are water-cooled to approximately room temperature. The hydrogen excited by the filament flows through a collision cell en route to a high vacuum chamber evacuated with two turbopumps to a base pressure of 10^{-7} torr (1 torr = 133.322 Pa) when the hydrogen flow is stopped. The collision cell is a 3″ long piece of 3/4″ (1 inch = 25.4 mm) inner diameter stainless steel tubing with a 90° bend. The mean free path at this pressure is on the order of 10 cm, so most of the thermalizing collisions occur with the room temperature chamber walls; thus, the bend in the cell promotes collisions with the chamber walls, thereby promoting relaxation. Because the rotational levels are much more closely spaced than the vibrational levels ($2B \approx 100$ cm^{-1}, $\omega \approx 4000$ cm^{-1}), collisions can almost completely relax the rotational excitation while still leaving a measurably high concentration in vibrationally excited states.

The collision cell is connected to the main vacuum chamber near the ionization region of a Wiley–McLaren time-of-flight mass spectrometer (19). A pulsed, tunable UV laser (see below) is focused in the ionization region, and hydrogen molecules that intersect the laser focus are ionized via (2 + 1) REMPI on the $E,F\,^1\Sigma_g^+ - X\,^1\Sigma_g^+$ band of interest. The resulting photoions are detected with the mass spectrometer, and he signal is corrected for variation in laser power. Concen - trations are measured by recording the ion current as the laser is scanned over the Doppler profile and then integrating the spectral line. Line strengths are then extracted by comparing the measured concentrations to the expected concentrations.

Resonant ionization of these three different isotopes and four different vibrational manifolds requires pulsed, tunable UV light in the wavelength range 207–234 nm. Three different frequency-mixing schemes were implemented to cover this range. All schemes involved a dye laser pumped by the second or third harmonic of a Nd:YAG laser. For the reddest wavelength range (229–234 nm), corresponding to $H_2(v'' = 3)$ and $HD(v'' = 4)$, a frequency-doubling scheme was employed. For the bluest wavelength range (207–215 nm), corresponding to $H_2(v'' = 1)$, $HD(v'' = 1)$ and $D_2(v'' = 1, 2)$, a frequency-tripling scheme was used. For the intermediate range, a less common 355 nm mixing scheme was employed. In this technique, the Nd:YAG laser is frequency doubled and tripled, and the residual second harmonic pumps the dye laser. The dye laser fundamental is then frequency summed with the Nd:YAG third harmonic to produce UV light in the range 216–229 nm. These techniques all produce approximately 1 mJ of UV light in a 5 ns pulse.

Theoretical methods

The present study follows the same computational steps as described earlier. (13, 20, 21). The two-photon transition moment (M_{fo}) is given by

$$[1] \qquad M_{fo} = \sum_i \frac{\langle f|\bar{r}\cdot\hat{\varepsilon}|i\rangle\langle i|\bar{r}\cdot\hat{\varepsilon}|o\rangle}{(E_i - E_o - \hbar\omega)}$$

The summation is over all rovibrational states that can be coupled to the initial and final states by dipole-allowed transitions. In total, 124 intermediate states are used in the summation. For the four lowest electronic states that are dipole coupled to the ground state (i.e., the $B\,^1\Sigma_u^+$, $C\,^1\Pi_u$, $B'\,^1\Sigma_u^+$, and $D\,^1\Pi_u$ states) explicit summation is carried out over their vibrational levels. For the remainder, a nuclear sudden approximation (21) is used. The calculation of the vibrational wave functions of the X state is based on the adiabatic potential compiled by Schwartz and Le Roy (22). For the (E,F), B, C, B′, and D states, the calculations are based on the adiabatic potentials of Wolniewcz and Dressler (23, 24).

Fig. 1. Boltzmann plots of the measured concentrations in H_2. The rotational and nuclear spin degeneracies are represented by g_J and g_N, respectively.

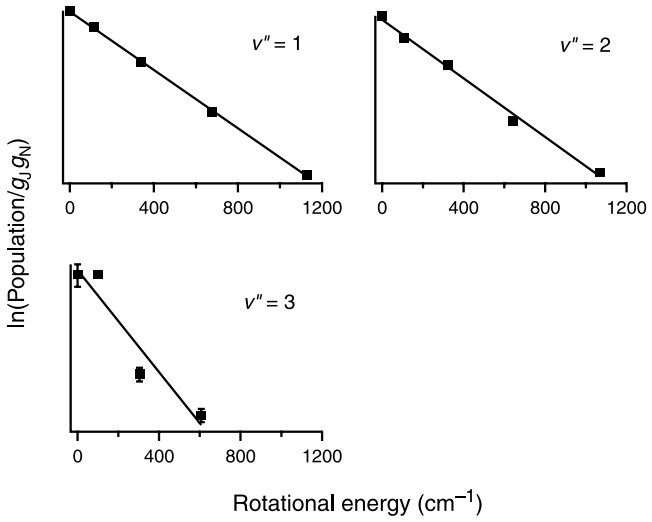

Fig. 2. Boltzmann plots of the measured concentrations in HD. The rotational and nuclear spin degeneracies are represented by g_J and g_N, respectively.

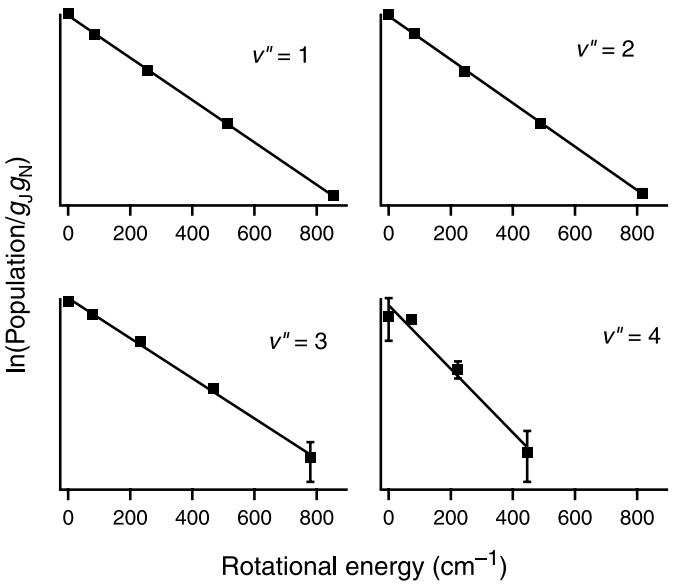

Results and discussion

Relative line strengths are extracted from the concentration measurements by comparing the measured concentrations to a Boltzmann distribution. This hot filament excitation technique is known to produce relative rotational concentrations that are well described by a Boltzmann distribution at slightly above room temperature (15–18). As the rotational line strengths are expected to be independent of J'', the experimentally determined concentrations are taken to be proportional to the area under the Doppler profile, without requiring a line strength correction. If this method of analysis returns an experimental distribution of concentrations that is well described by a Boltzmann distribution at slightly above room temperature then it represents experimental confirmation that the relative rotational line strengths are independent of J'' to within the experimental uncertainty. The experimental error is estimated to be approximately 10%. Further experimental determination of the relative rotational line strengths is impossible because the rotational temperature of the sample is not known precisely. Experimental determination of the v'' dependence of the line strengths is similarly impossible because the vibrational temperature of the sample is unknown.

It is important to note that the measured concentrations have been corrected for differences in the nuclear spin degeneracy. Because of these nuclear statistics, the concentration of $H_2(J'' = \text{odd})$ (*ortho*-hydrogen) is three times larger than the concentration of $H_2(J'' = \text{even})$ (*para*-hydrogen). To prepare the Boltzmann plots, the concentrations of $H_2(J'' = \text{odd})$ have been divided by three; similarly, the concentrations of $D_2(J'' = \text{even})$ have been divided by two. No correction is necessary for HD because the nuclei are not identical.

Boltzmann plots of the measured concentrations are presented in Figs. 1–3, and the resulting rotational temperatures are presented in Table 1. The Boltzmann plots present the natural logarithm of the population divided by the rotational degeneracy ($g_J = 2J''+1$) and the nuclear spin degeneracy

Fig. 3. Boltzmann plots of the measured concentrations in D_2. The rotational and nuclear spin degeneracies are represented by g_J and g_N, respectively.

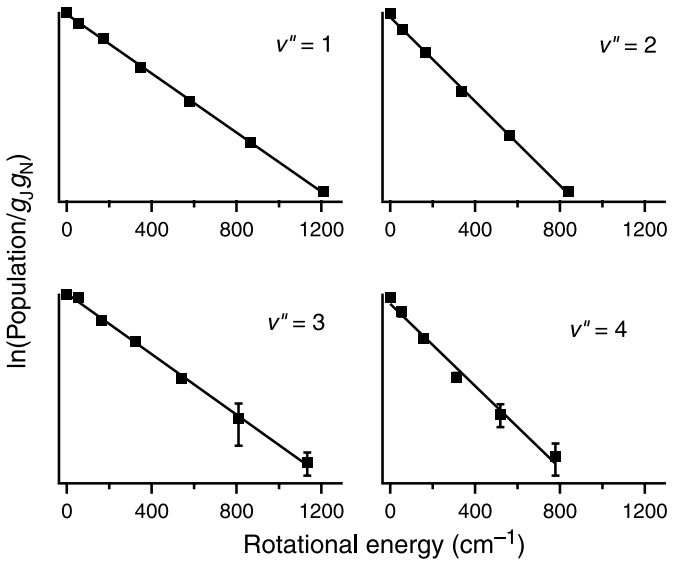

Table 1. Rotational temperatures (K) of each vibrational manifold.

v''	H_2	HD	D_2
1	317 (4)	308 (2)	312 (4)
2	323 (15)	314 (3)	308 (6)
3	342 (77)	302 (9)	316 (6)
4		340 (38)	323 (17)

Note: Uncertainties (one standard deviation) are listed in parentheses.

Table 2. Theoretical values of $|M_{fo}|^2$ for $E,F^1\Sigma_g^+(v' = 0, J' = J'') - X^1\Sigma_g^+(v'', J'')$ (2 + 1) REMPI transitions in H_2 (au).

J''	$v''=0$	$v''=1$	$v''=2$	$v''=3$	$v''=4$	$v''=5$	$v''=6$
0	**9.12**	**26.36**	**29.38**	**16.24**	4.73	0.71	0.07
1	9.15	**26.47**	**29.54**	**16.36**	4.78		
2	**9.20**	**26.61**	**29.71**	**16.45**	4.80		
3	**9.26**	**26.83**	**29.98**	**16.62**	4.85		
4	**9.34**	**27.12**	**30.36**	16.84	4.92		
5	9.44	**27.48**	**30.82**	17.13	5.01		
6	**9.56**	**27.91**	**31.39**	17.48	5.12		
7	**9.68**	**28.34**	**31.97**	17.85	5.24		
8	**9.85**	**28.97**	32.83	18.39	5.42		
9	**10.02**	**29.60**	33.70	18.91	5.66		
10	**10.18**	**30.28**	34.61	19.58	5.92		
11	**10.36**	**31.06**	35.73	20.38	6.16		
12	**9.66**	29.82	34.00	20.06	6.44		
13	**10.89**	**32.87**	38.17	22.03	6.92		
14	**8.77**	26.38	31.06	16.72	4.55		
15	**11.62**	35.47	41.38	23.93	7.79		
16	11.49	35.21	42.06	24.48	7.53		
17	11.65	37.00	42.15	25.84	10.20		
18	12.05	38.84	48.56	29.87	9.82		
19	9.26	31.62	39.00	22.53	5.52		
20	6.28	25.59	38.94	36.06	23.62		
21	8.63	33.58	49.84	39.62	16.72		

Note: Rotational line strengths that have been confirmed by the current or previous (12) experiment are listed in bold.

Table 3. Theoretical values of $|M_{fo}|^2$ for $E,F^1\Sigma_g^+(v' = 0, J' = J'') - X^1\Sigma_g^+(v'', J'')$ (2 + 1) REMPI transitions in HD (au).

J''	$v''=0$	$v''=1$	$v''=2$	$v''=3$	$v''=4$	$v''=5$	$v''=6$
0	**6.87**	**22.12**	**28.50**	**19.07**	**7.18**	1.53	0.18
1	**6.89**	**22.20**	**28.62**	**19.18**	**7.23**		
2	**6.91**	**22.28**	**28.74**	**19.26**	**7.26**		
3	**6.95**	**22.41**	**28.92**	**19.40**	**7.31**		
4	**6.99**	**22.59**	**29.19**	**19.60**	7.39		
5	**7.04**	**22.81**	**29.53**	19.84	7.48		
6	**7.11**	**23.07**	**29.92**	20.14	7.61		
7	**7.19**	**23.37**	**30.39**	20.49	7.74		
8	**7.27**	**23.72**	**30.92**	20.90	7.91		
9	**7.36**	**24.10**	31.53	21.37	8.10		
10	**7.45**	**24.51**	32.20	21.90	8.32		
11	**7.56**	**24.97**	32.93	22.49	8.60		
12	**7.66**	25.46	33.76	23.16	8.91		
13	**7.84**	26.04	34.53	23.59	9.28		
14	7.88	26.53	35.63	24.36	9.58		
15	7.93	27.10	36.41	25.56	10.07		
16	8.32	28.07	37.74	26.21	10.38		
17	3.92	14.93	19.61	14.83	6.88		
18	8.85	30.18	41.00	28.23	11.05		
19	8.65	30.65	41.49	29.12	11.65		
20	7.54	27.60	38.38	28.86	13.60		
21	9.08	33.11	47.47	34.67	14.17		
22	8.72	31.24	45.91	32.88	11.49		
23	5.10	18.91	33.76	34.97	21.59		
24	6.51	27.16	46.20	43.73	26.10		

Note: Rotational line strengths that have been confirmed by the current or previous (12) experiment are listed in bold.

Table 4. Theoretical values of $|M_{fo}|^2$ for $E,F^1\Sigma_g^+(v' = 0, J' = J'') - X^1\Sigma_g^+(v'', J'')$ (2 + 1) REMPI transitions in D_2 (au).

J''	$v''=0$	$v''=1$	$v''=2$	$v''=3$	$v''=4$	$v''=5$	$v''=6$
0	**4.25**	**16.33**	**25.48**	**22.15**	**11.49**	3.75	0.74
1	**4.29**	**16.23**	**25.63**	**22.17**	**11.55**		
2	**4.30**	**16.26**	**25.70**	**22.23**	**11.58**		
3	**4.31**	**16.32**	**25.81**	**22.33**	**11.63**		
4	**4.33**	**16.38**	**25.96**	**22.48**	**11.71**		
5	**4.35**	**16.48**	**26.15**	**22.66**	**11.81**		
6	**4.38**	**16.60**	**26.37**	**22.88**	11.94		
7	**4.41**	**16.77**	**26.64**	23.14	12.07		
8	**4.44**	**16.92**	**26.93**	23.44	12.25		
9	**4.47**	**17.10**	**27.27**	23.78	12.44		
10	**4.51**	**17.35**	**27.65**	24.16	12.66		
11	**4.55**	**17.50**	**28.06**	24.58	12.90		
12	**4.59**	**17.72**	28.51	25.04	13.18		
13	**4.64**	**17.96**	28.99	25.55	13.48		
14	**4.68**	**18.21**	29.52	26.10	13.81		
15	**4.72**	18.44	30.05	26.67	14.17		
16	**4.80**	18.79	30.63	27.30	14.47		
17	**4.79**	18.99	31.32	28.11	15.04		
18	4.86	19.32	31.95	28.81	15.54		
19	4.99	20.20	32.65	29.18	15.95		
20	5.02	20.07	33.39	30.31	16.58		
21	5.17	20.57	34.08	30.61	16.54		
22	5.21	21.03	35.25	32.04	17.58		
23	5.21	21.34	36.01	33.11	18.41		
24	4.97	20.82	36.12	33.65	18.72		
25	5.38	22.54	38.78	35.93	19.95		
26	5.82	26.10	43.56	40.66	21.38		
27	3.28	14.45	27.09	28.33	18.29		
28	5.27	24.56	47.57	51.92	34.37		
29	5.46	23.57	49.14	50.80	33.03		
30	4.71	19.57	39.98	41.56	22.77		

Note: Rotational line strengths that have been confirmed by the current or previous (12) experiment are listed in bold.

(g_N) as a function of rotational energy; they are fit to a straight line whose slope depends inversely on temperature. The measured rotational temperatures all lie in the expected range, indicating that the relative rotational line strengths are independent of J'' within the 10% experimental uncertainty for the rotational states measured here. This finding is confirmed by the theoretical values of the square of the two-photon transition moment $|M_{fo}|^2$, which are presented in Tables 2–4. For completeness, previously determined $|M_{fo}|^2$ are also presented in Tables 2–4 (12). The vibrational dependence of the line strengths is known theoretically, so the theoretical line strengths presented include the dependence on v''. Although the current experiment is insensitive to vibrational line strengths, a previous measurement of the vibrational line strengths is in good agreement with the theory for $v'' = 1, 2$ (12). Relative rotational line strengths that have been measured here or previously and shown to be in good agreement with theory are indicated in the tables. We find virtually no transitions in which experimental line strengths significantly disagree with the theoretical ones; the only exceptions occur at very high rotational levels ($J'' \sim 15$) of the lowest vibrational manifold. We note that the numbers presented here are line strengths, so concentrations should be

Table 5. Calculated values of frequencies for $E,F^1\Sigma_g^+(v' = 0, J' = J'') - X^1\Sigma_g^+$ (v'', J'') transitions in H_2 (cm^{-1}).

J''	$v'' = 0$	$v'' = 1$	$v'' = 2$	$v'' = 3$	$v'' = 4$	$v'' = 5$	$v'' = 6$
0	99 138.66	94 976.69	91 050.32	87 353.92	83 885.39	80 643.32	77 629.10
1	99 083.59	94 927.54	91 006.96	87 316.25	83 853.36		
2	98 974.02	94 829.76	90 920.72	87 241.36	83 789.76		
3	98 811.05	94 684.40	90 792.58	87 130.16	83 695.40		
4	98 596.29	94 492.94	90 623.93	86 983.96	83 571.52		
5	98 331.79	94 257.30	90 416.57	86 804.41	83 419.65		
6	98 019.96	93 979.73	90 172.58	86 593.47	83 241.62		
7	97 663.51	93 662.73	89 894.30	86 353.29	83 039.44		
8	97 265.46	93 309.12	89 584.34	86 086.30	82 815.36		
9	96 828.75	92 921.59	89 245.22	85 794.79	82 571.53		
10	96 356.68	92 503.20	88 879.78	85 481.40	82 310.40		
11	95 851.96	92 056.40	88 490.32	85 148.15	82 033.85		
12	95 316.32	91 582.67	88 078.05	84 796.11	81 742.80		
13	94 757.35	91 089.34	87 650.27	84 432.19	81 444.02		
14	94 185.04	90 586.18	87 215.12	84 065.80	81 146.82		
15	93 565.52	90 039.07	86 742.61	83 662.51	80 816.68		
16	92 947.40	89 496.42	86 276.01	83 270.13	80 501.33		
17	92 280.13	88 907.51	85 768.07	82 838.91	80 152.99		
18	91 637.43	88 345.91	85 289.69	82 440.65	79 840.66		
19	91 012.34	87 804.52	84 830.45	82 068.00	79 558.30		
20	90 200.23	87 078.66	84 192.28	81 518.58	79 103.63		
21	89 568.05	86 535.21	83 742.06	81 158.69	78 841.96		

Table 6. Calculated values of frequencies for $E,F^1\Sigma_g^+(v' = 0, J' = J'') - X^1\Sigma_g^+$ (v'', J'') transitions in HD (cm^{-1}).

J''	$v'' = 0$	$v'' = 1$	$v'' = 2$	$v'' = 3$	$v'' = 4$	$v'' = 5$	$v'' = 6$
0	99 303.14	95 670.43	92 215.25	88 933.81	85 824.09	82 884.45	80 114.85
1	99 261.70	95 632.85	92 181.45	88 903.73	85 797.70		
2	99 179.16	95 558.00	92 114.14	88 843.84	85 745.17		
3	99 056.11	95 446.45	92 013.86	88 754.66	85 667.00		
4	98 893.51	95 299.11	91 881.46	88 636.98	85 563.91		
5	98 692.52	95 117.05	91 717.97	88 491.77	85 436.85		
6	98 454.59	94 901.66	91 524.66	88 320.24	85 286.92		
7	98 181.34	94 654.45	91 302.97	88 123.73	85 115.40		
8	97 874.55	94 377.08	91 054.45	87 903.71	84 923.66		
9	97 536.15	94 071.36	90 780.80	87 661.76	84 713.18		
10	97 168.13	93 739.16	90 483.76	87 399.52	84 485.48		
11	96 772.55	93 382.39	90 165.12	87 118.64	84 242.16		
12	96 351.44	93 002.95	89 826.63	86 820.79	83 984.73		
13	95 906.80	92 602.69	89 470.03	86 507.56	83 714.72		
14	95 440.80	92 183.62	89 097.20	86 180.71	83 433.78		
15	94 954.91	91 747.06	88 709.35	85 841.34	83 142.93		
16	94 451.72	91 295.49	88 308.83	85 491.68	82 844.34		
17	93 921.18	90 818.72	87 885.34	85 121.34	82 527.55		
18	93 397.19	90 350.52	87 472.54	84 763.90	82 226.09		
19	92 852.79	89 863.82	87 043.30	84 392.17	81 912.70		
20	92 277.65	89 348.19	86 587.08	83 995.59	81 576.80		
21	91 715.55	88 847.34	86 147.53	83 617.77	81 262.02		
22	91 156.66	88 351.36	85 714.69	83 248.79	80 958.45		
23	90 469.91	87 729.13	85 157.39	82 757.48	80 535.06		
24	89 916.75	87 242.08	84 737.07	82 405.34	80 253.47		

obtained by dividing measured signal levels by these numbers. This convention was not followed in some previous publications in which inverse line strengths were reported (12).

Tables 5–7 present calculated frequencies for these transitions using the adiabatic potentials of the X state (22) and the (E,F) state (23). The transition frequencies for D_2 in Table 7 have been previously published (25). Due to the lack

Table 7. Calculated values of frequencies for $E,F^1\Sigma_g^+(v' = 0, J' = J'') - X^1\Sigma_g^+$ (v'', J'') transitions in D_2 (cm^{-1}).

J''	$v'' = 0$	$v'' = 1$	$v'' = 2$	$v'' = 3$	$v'' = 4$	$v'' = 5$	$v'' = 6$
0	99 460.11	96 466.56	93 592.10	90 834.67	88 192.60	85 664.71	83 250.28
1	99 432.38	96 440.94	93 568.56	90 813.16	88 173.11		
2	99 377.07	96 389.83	93 521.59	90 770.28	88 134.26		
3	99 294.45	96 313.52	93 451.47	90 706.26	88 076.28		
4	99 184.95	96 212.39	93 358.57	90 621.47	87 999.52		
5	99 049.10	96 086.96	93 243.38	90 516.37	87 904.41		
6	98 887.58	95 937.87	93 106.51	90 391.55	87 791.51		
7	98 701.14	95 765.83	92 948.64	90 247.65	87 661.44		
8	98 490.65	95 571.69	92 770.56	90 085.42	87 514.91		
9	98 257.06	95 356.32	92 573.12	89 905.67	87 352.68		
10	98 001.35	95 120.67	92 357.20	89 709.24	87 175.56		
11	97 724.60	94 865.76	92 123.78	89 497.04	86 984.40		
12	97 427.90	94 592.62	91 873.83	89 270.00	86 780.09		
13	97 112.36	94 302.29	91 608.33	89 029.05	86 563.51		
14	96 779.11	93 995.85	91 328.31	88 775.16	86 335.57		
15	96 429.29	93 674.37	91 034.76	88 509.27	86 097.16		
16	96 064.01	93 338.89	90 728.68	88 232.30	85 849.17		
17	95 684.37	92 990.45	90 411.04	87 945.20	85 592.46		
18	95 291.43	92 630.04	90 082.77	87 648.82	85 327.87		
19	94 886.25	92 258.65	89 744.81	87 344.07	85 056.25		
20	94 469.70	91 877.12	89 397.93	87 031.65	84 778.25		
21	94 043.03	91 486.60	89 043.26	86 712.65	84 494.94		
22	93 606.25	91 087.08	88 680.70	86 386.94	84 206.16		
23	93 161.66	90 680.80	88 312.46	86 056.69	83 914.04		
24	92 704.86	90 263.30	87 934.06	85 717.37	83 614.06		
25	92 245.48	89 844.18	87 555.05	85 378.52	83 315.73		
26	91 781.28	89 421.15	87 173.11	85 037.82	83 016.74		
27	91 276.13	88 958.06	86 752.06	84 659.05	82 680.91		
28	90 809.57	88 534.42	86 371.42	84 321.74	82 387.77		
29	90 337.70	88 106.30	85 987.22	83 981.95	82 093.46		
30	89 886.44	87 699.63	85 625.40	83 665.63	81 823.98		

of nonadiabatic and relativistic corrections, these frequencies are not of spectroscopic accuracy. For the X state, nonadiabatic corrections have been reported by Schwartz and Le Roy (22). However, similar calculations have not been done for the (E,F) state. To be consistent, the present calculation chooses to use the adiabatic approximation and does not incorporate nonadiabatic corrections for the X state. The calculated frequencies are expected to be of similar accuracy as the D_2 data where extensive comparisons with experiment have been made (25). Most differences are within a few cm^{-1}. The tabulated frequencies should be sufficiently accurate to allow determination of line positions in future experiments. We note that the simple appearance of these spectra (the spacing between rotational lines grows at a roughly constant rate in each vibrational manifold) will facilitate line identification. As the two-photon transition moments do not depend on the separation between the energy levels, any inaccuracies in the calculated line positions will not affect the accuracy of the line strength calculations.

Conclusions

Line strengths for many $E,F^1\Sigma_g^+(v' = 0, J' = J'') - X^1\Sigma_g^+$ (v'', J'') (2 + 1) REMPI transitions in H_2, HD, and D_2 are presented. Experimental and theoretical values for these line strengths show good agreement, and the line strengths are found to depend strongly on v'' but only weakly on J''. Knowledge of these line strengths should be useful whenever rovibrationally state resolved concentrations of molecular hydrogen are of interest, particularly in the study of the nascent populations of gas-phase or gas-surface interactions.

Acknowledgments

The work of the Stanford group is supported by the National Science Foundation under grant number 0242103.

References

1. T. Lyman. Astrophys. J. **23**, 181 (1906).
2. S. Werner. Proc. Roy. Soc. London Ser. A, **113**, 107 (1926).
3. G. Herzberg and L.L. Howe. Can. J. Phys. **37**, 636 (1959).
4. E.E. Marinero, C.T. Rettner, and R.N. Zare. J. Chem. Phys. **80**, 4142 (1984).
5. D.A.V. Kliner, K.-D. Rinnen, M.A. Buntine, D.E. Adelman, and R.N. Zare. J. Chem. Phys. **95**, 1663 (1991).
6. A.E. Pomerantz, F. Ausfelder, R.N. Zare, S.C. Althorpe, F.J. Aoiz, L. Bañares, and J.F. Castillo. J. Chem. Phys. **120**, 3244 (2004).
7. F. Ausfelder, A.E. Pomerantz, R.N. Zare, S.C. Althorpe, F.J. Aoiz, L. Bañares, and J.F. Castillo. J. Chem. Phys. **120**, 3255 (2004).

8. G. Požgainer, K.D. Rendulic, and A. Winkler. Surf. Sci. **307–309**, 344 (1994).
9. G. Eilmsteiner and A. Winkler. Surf. Sci. **366**, L750 (1996).
10. G.D. Kubiak, G.O. Sitz, and R.N. Zare. J. Chem. Phys. **83**, 2538 (1985).
11. G. Požgainer, L. Windholz, and A. Winkler. Meas. Sci. Technol. **5**, 947 (1994).
12. K.-D. Rinnen, M.A. Buntine, D.A.V. Kliner, R.N. Zare, and W.M. Huo. J. Chem. Phys. **95**, 214 (1991).
13. W.M. Huo, K.-D. Rinnen, and R.N. Zare. J. Chem. Phys. **95**, 205 (1991).
14. E.E. Marinero, R. Vasudev, and R.N. Zare. J. Chem. Phys. **78**, 692 (1983).
15. R.I. Hall, I. Cadež, M. Landau, F. Pichou, and C. Schermann. Phys. Rev. Lett. **60**, 337 (1988).
16. P.J. Eenshuistra, J.H.M. Bonnie, J. Los, and H.J. Hopman. Phys. Rev. Lett. **60**, 341 (1988).
17. D.C. Robie, L.E. Jusinski, and W.K. Bischel. Appl. Phys. Lett. **56**, 722 (1990).
18. F. Fernández-Alonso, B.D. Bean, J.D. Ayers, A.E. Pomerantz, and R.N. Zare. Z. Phys. Chem. (Muenchen), **214**, 1167 (2000).
19. W.C. Wiley and I.H. McLaren. Rev. Sci. Instrum. **26**, 1150 (1955).
20. W.M. Huo, and R.L. Jaffe. Chem. Phys. Lett. **101**, 463 (1983).
21. K.-D. Rinnen, D.A.V. Kliner, R.N. Zare, and W.M. Huo. Isr. J. Chem. **29**, 369 (1989).
22. C. Schwartz and R.J. Le Roy. J. Mol. Spectrosc. **121**, 420 (1987).
23. L. Wolniewicz and K. Dressler. J. Chem. Phys. **82**, 3292 (1985).
24. L. Wolniewicz and K. Dressler. J. Chem. Phys. **88**, 3861 (1988).
25. A.J. Heck, W.M. Huo, R.N. Zare, and D.W. Chandler. J. Mol. Spectrosc. **173**, 452 (1995).